Applications and Applied Mathematics: An International Journal (AAM)

Volume 12 | Issue 1 Article 35

6-2017

Effect of Buoyancy and Magnetic Field on Unsteady Convective Diusion of Solute in a Boussinesq Stokes Suspension Bounded by Porous Beds

Nirmala P. Ratchagar
Annamalai University

R. Vijayakumar
Annamalai University

Available at
http://pvamu.edu/aam
Appl. Appl. Math.
ISSN: 1932-9466
Vol. 12, Issue 1 (June 2017), pp. 540 – 563

Applications and Applied Mathematics:
An International Journal
(AAM)

Effect of Buoyancy and Magnetic Field on Unsteady Convective Diffusion of Solute in a Boussinesq Stokes Suspension Bounded by Porous Beds

[1]Nirmala P. Ratchagar & [2]R. Vijayakumar

[1]Department of Mathematics
Annamalai University
Annamalainagar - 608 002, India
nirmalapasala@yahoo.co.in
&
[2]Mathematics Section
Faculty of Engineering and Technology
Annamalai University
Annamalainagar - 608 002, India
rathirath_viji@yahoo.co.in

Received: July 16, 2016; Accepted: February 22, 2017

Abstract

Hydromagnetic free and forced convection in a parallel plate channel bounded by porous bed and transverse magnetic field has been considered. When there is a uniform axial temperature variation along the walls, the primary flow shows incipient flow reversal at the upper plate for an increase in temperature along that plate. Similarly flow reversal at the lower plate occurs with a decrease in temperature along that plate. The magnetic field, arising as a body couple in the governing equations is shown to increase the axis dispersion coefficient. The effect of various physical parameters such as Hartmann number, Grashof number, porous parameter and couple stress parameter on the velocity, temperature and dispersion coefficient, mean concentration, skin friction coefficient and Nusselt numbers are computed and analyzed through graphs.

Keywords: Hartmann number; Heat and mass transfer; Magnetohydrodynamic; couple stress fluid; generalized dispersion model

MSC 2010 No.: 76S05, 76W05, 76D05

1. Introduction

The external regulation of dispersion in plane parallel flow is very important from the point of view of its applications in biomechanical, chemical engineering and in many industrial problems. One way of regulating dispersion is by means of influencing the flow by appropriate thermal means at the boundaries. Miscible dispersion of passive solute also depends on the fluid solvent.

Many applications involve solvents with micron sized suspended particles and these results in change of solvent viscosity. The particles also have relative spin with respect to the solvent. Stoke's couple stress fluid is one such fluid, which models suspensions. The unsteady convective diffusions of passive solute in this fluid has been analyzed by Rudraiah et al. (1986). The bounding walls and their problem are assumed to be permeable.

Lighthill (1966) obtained the exact solution of the unsteady convection diffusion equation, which is asymptotically valid for small time. Chatwin (1971) also studied the theory for large time by the Laplace transform technique. Barton (1986) has resolved certain technical difficulties in the Aris (1956) method of moments and obtained the solutions of the second and third moments equations of the distribution of the solute, valid for all time. However, Sankarasubramanian and Gill (1973) have developed an analytical method to analyze the transient dispersion of a non-uniform initial distribution, called generalized dispersion in a channel.

The effect of buoyancy forces caused by a density difference due to concentration difference of a solvent in a straight horizontal pipe studied by Erdogan and Chatwin (1967). Barton and Stokes (1986) computed shear dispersion in parallel flow numerically. Mazumder (1979) studied the dispersion of solute in the combined free and forced convective laminar flow between two parallel plates in presence of uniform axial temperature variation along the channel walls, for asymptotically large time and found that effective Taylor diffusion coefficient increases with the Grashof number. Bestman (1983) studied the unsteady low Reynolds number flow in a heated tube of slowly varying section. In that analysis the effect of forced and free convection heat transfer on flow in an axisymmetric tube whose radius varied slowly in the axial direction was addressed.

Siddheshwar and Thangaraj (2005) investigated the dispersion of solute in a fully developed flow of a Boussinesq Stokes suspension through a parallel channel with axial variation of temperature along the bounding walls. Sivasankaran (2007) examined the effect of variable thermal conductivity on buoyant convection in a cavity with internal heat generation. Kafoussias et al. (2008) described the two dimensional steady and laminar free-forced convective boundary layer flow of a biomagnetic fluid over a semi infinite vertical hot plate under the action of a localized magnetic field.

Tzirtzilakis et al. (2010) studied the forced and free convective boundary layer flow of a magnetic fluid over a flat plate under the action of a localized magnetic field. Sibanda and Makinde (2010) investigated the MHD flow and heat transfer past a rotating disk in a porous medium with ohmic

heating and viscous dissipation. Rashidi et al. (2012) applied MHD flow in medicine science. They studied the dual control mechanisms of transverse magnetic field and porous media filtration in a buoyancy-driven blood flow regime in a vertical pipe, as a model of a blood separation configuration.

Makinde et al. (2013) described the buoyancy effects on MHD stagnation point flow and heat transfer of a nanofluid past a convectively heated stretching/ shrinking sheet. Bhuvaneswari and Sivasankaran (2014) investigated the free convection flow in an inclined plate with variable thermal conductivity by scaling group transformations. Rundora and Makinde (2015) investigate the combined effects of suction/injection and Navier slip at the channel walls on the heat transfer characteristics in such flows. Chinyoka and Makinde (2015) studied the unsteady flow of a reactive variable viscosity third-grade fluid between two parallel porous plates filled with a porous medium and acted upon by both nonconstant pressure and buoyancy effects. Both the left-hand side and right-hand side walls of the channel are subjected to asymmetric convective heat exchange with the ambient and allow for uniform suction/injection in the transverse direction.

The objective of the present chapter is to study the dispersion of a solute in combined free and forced convective laminar flow through a horizontal channel bounded by porous beds with uniform axial temperature variation along the walls, using generalized dispersion of a solute (Gill and Sankarasubramanian (1970)).

2. Mathematical Formulation

For a steady fully developed laminar flow, the velocity u in the x direction is a function of y only. Consider the combined free and forced convective laminar flow of a viscous incompressible fluid bounded by porous layers, separated by a distance $2h$ apart, in the presence of a uniform linear axial temperature variation along the channel.

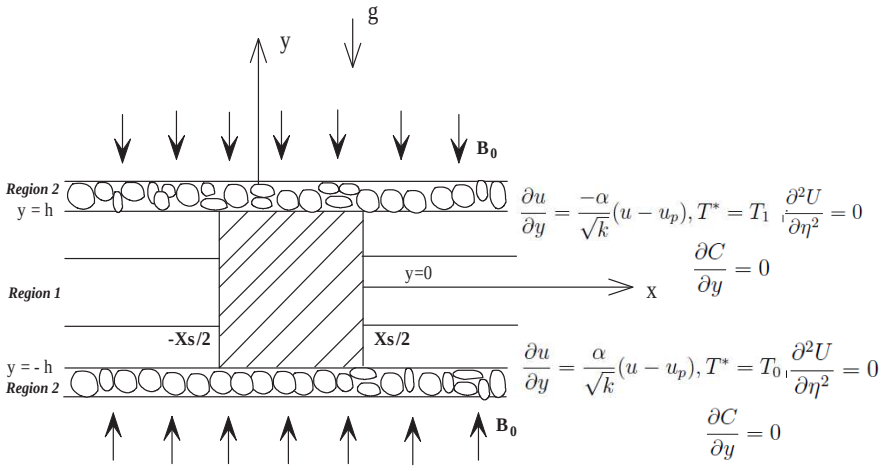

Figure 1. Physical Configuration

The equations governing the flow of a couple stress fluid are given by Srinivasacharya et al.

(2011).

Region 1: Fluid Film

Conservation of mass for an incompressible flow

$$\nabla \cdot \vec{V} = 0, \tag{1}$$

Conservation of momentum

$$\rho \frac{D\vec{V}}{Dt} = -\nabla p + \mu \nabla^2 \vec{V} - \lambda \nabla^4 \vec{V} + J \times B + \rho g, \tag{2}$$

Conservation of energy

$$\begin{aligned} \rho C_p \frac{D\vec{T}}{Dt} &= K_T \nabla^2 \vec{T} + \mu[(\nabla \vec{V}) : (\nabla \vec{V})^T + (\nabla \vec{V}) : (\nabla \vec{V})] \\ &+4\lambda[(\nabla \vec{\omega}) : (\nabla \vec{\omega})^T] + 4\lambda'[(\nabla \vec{\omega}) : (\nabla \vec{\omega})^T] + \frac{J.J}{\sigma_0}, \end{aligned} \tag{3}$$

Conservation of species

$$\frac{D\vec{C}}{Dt} = D\nabla^2 \vec{C}. \tag{4}$$

Region 2: Porous Tissue

Conservation of mass for an incompressible flow

$$\nabla \cdot \vec{V_p} = 0, \tag{5}$$

Conservation of momentum

$$\rho \frac{D\vec{V_p}}{Dt} = -\nabla p + \mu \nabla^2 \vec{V_p} - \frac{\mu}{k}(1+\beta)\vec{V_p} + \rho g, \tag{6}$$

where $\frac{D}{Dt} = \frac{\partial}{\partial t} + \vec{V}.\nabla$ is the material derivative, $\vec{V} = (u^*, v^*, 0)$ is the velocity vector, ρ the blood density, μ is the dynamic viscosity of the blood, $\vec{T}$ is the temperature of the blood, λ and λ' are the couple stress parameter, C_p is the specific heat at the constant pressure, K_T is the thermal conductivity, $\vec{\omega}$ is the rotation vector, $\vec{C}$ is the concentration, D is the molecular diffusivity, k is the permeability parameter of porous medium and g is gravity.

In deriving the governing equation and the corresponding boundary conditions the following assumptions are made.

- Blood is treated as a couple stress fluid (non-Newtonian).
- Flow region may be classified into two sub-regions fluid film and porous tissue(Figure 1).
- The biomagnetic fluid flow is laminar, steady, unidirectional and incompressible.
- The induced magnetic field and the electric field produced by the motion of blood are negligible (since blood has low magnetic Reynolds number)

- A uniform magnetic field B_0 is applied in the $y-$direction to the flow of blood.
- The effect of viscous dissipation and Joule heating are considered in the energy equation.
- The Boussinesq approximation is applied.
- Concentration C is introduced as a slug which is a function of time (t) and coordinates x and y.

Under the above stated assumptions, equations (1) and (6) reduces to

Region 1: Fluid Film

$$\frac{\partial u}{\partial x} = 0,$$

$$0 = -\frac{\partial p^*}{\partial x} + \mu\frac{\partial^2 u}{\partial y^2} - \lambda\frac{\partial^4 u}{\partial y^4} - B_0^2\sigma_0 u, \tag{7}$$

$$0 = -\frac{\partial p^*}{\partial y} - \rho g, \tag{8}$$

and energy equation (3) becomes

$$0 = K_T\frac{\partial^2 T^*}{\partial y^2} + \mu\left(\frac{\partial u}{\partial y}\right)^2 + \lambda\left(\frac{\partial^2 u}{\partial y^2}\right)^2 + \sigma_0 B_0^2 u^2. \tag{9}$$

The concentration C satisfying the convective diffusion equation (4) gives

$$\frac{\partial C}{\partial t} + u\frac{\partial C}{\partial x} = D\left(\frac{\partial^2 C}{\partial x^2} + \frac{\partial^2 C}{\partial y^2}\right). \tag{10}$$

Region 2: Porous Tissue

$$\frac{\partial u_p}{\partial x} = 0,$$

$$0 = -\frac{\partial p^*}{\partial x} - \frac{\mu(1+\beta_1)}{k}u_p, \tag{11}$$

$$0 = -\frac{\partial p^*}{\partial y} - \rho g, \tag{12}$$

The boundary conditions on the velocity and temperature are,

$$\frac{\partial u}{\partial y} = \frac{-\alpha}{\sqrt{k}}(u - u_p), T^* = T_1 \quad at \quad y = h, \tag{13}$$

$$\frac{\partial u}{\partial y} = \frac{\alpha}{\sqrt{k}}(u - u_p), T^* = T_0 \quad at \quad y = -h, \tag{14}$$

The couple stress conditions,

$$\frac{\partial^2 u}{\partial y^2} = 0 \quad at \quad y = \pm h, \tag{15}$$

The initial and boundary conditions on concentration

$$C = \begin{cases} C_0, |x| \leq \dfrac{x_s}{2}, \\ \\ 0, |x| > \dfrac{x_s}{2}, \end{cases} \quad \text{at} \quad t = 0, \tag{16}$$

$$\frac{\partial C}{\partial y} = 0 \qquad \text{at} \quad y = \pm h, \tag{17}$$

$$C = \frac{\partial C}{\partial x} = 0 \qquad \text{at} \quad x = \infty, \tag{18}$$

where u represents the axial velocity of the blood, p^* is the pressure, B_0 the magnetic field, σ_0 is the electric conductivity of the blood, K_T is the the thermal conductivity, T^* is the temperature of blood, T_0 and T_1 are the temperatures at the lower and upper wall of blood. Equation (11) is the modified Darcy equation, modified in the sense of incompressible couple stress parameter, u_p is the Darcy velocity, α is the slip parameter and C_0 is the initial concentration of the initial slug input of length x_s.

Equations (13) and (14) are Beavers and Joseph (1967) slip condition at the lower and upper permeable surfaces. Equation (15) specifies the vanishing of couple stress at the boundaries. The term $\sigma_0 B_0^2 u$ in (7) represents the Lorentz force per unit volume and arises due to the electrical conductivity of the fluid, whereas the term $\sigma_0 B_0^2 u^2$ in (9) represents the Joule heating. These two terms arise due to the MHD (Cramer and Pai (1973) and Hughes and Young (1996)).

Assuming the uniform axial temperature variation along the walls, the temperature of the blood can be written as

$$T^* - T_0 = N'x + \phi(y), \tag{19}$$

where N' is a constant temperature gradient in the $x-$direction, $\phi(y)$ is certain function of temperature.

The equation of state under the Boussinesq approximation (Sekar and Raju (2013)) is assumed to be

$$\rho = \rho_0 \left(1 - \beta'(T^* - T_0)\right), \tag{20}$$

where ρ_0 is the density of a reference state and β' is the coefficient of volume expansion.

Substituting equations (19) and (20) in (8) and integrating with respect to y, we get

$$p^* = -\rho_0 g y + \rho_0 g \beta' N x y - \rho_0 g \beta' \int \phi(y) dy + \psi_1,$$

where $\psi_1 = \psi_1(x)$ is a $y-$ integration constant.

Differentiating with respect to x we get

$$\frac{\partial p^*}{\partial x} = \rho_0 g \beta' N y + \frac{\partial \psi_1}{\partial x}. \tag{21}$$

Substituting (21) in (7), we obtain

$$0 = -\rho_0 g\beta' N y - \frac{d\psi_1}{dx} + \mu\frac{\partial^2 u}{\partial y^2} - \lambda\frac{\partial^4 u}{\partial y^4} - \sigma_0 B_0^2 u. \tag{22}$$

Introducing the non-dimensional variables

$$U = \frac{uh}{\nu P_x}, U_p = \frac{u_p h}{\nu P_x}, \eta = \frac{y}{h}, P_x = \frac{-h^3}{\rho_0 \nu^2}\frac{d\psi_1}{dx}, T = \frac{T^* - T_0}{T_1 - T_0}.$$

Equations (9) and (22) in non-dimensional form are

Region 1: Fluid Film

$$\frac{\partial^4 U}{\partial \eta^4} - a^2\frac{\partial^2 U}{\partial \eta^2} + a^2 M^2 U = a^2(1 - G\eta), \tag{23}$$

and

$$\frac{a^2}{EcPr}\frac{\partial^2 T}{\partial \eta^2} + a^2\left(\frac{\partial U}{\partial \eta}\right)^2 + \frac{\partial^2 U}{\partial \eta^2}^2 + a^2 M^2 U^2 = 0. \tag{24}$$

Region 2: Porous Tissue

Integrating (12) with respect to y, then, substituting in (11) and using non-dimensional variables, we get

$$U_p = \frac{1}{\sigma^2(1 + \beta_1)}, \tag{25}$$

The boundary conditions of equations (13) to (15) in non-dimensional form are

$$\frac{\partial U}{\partial \eta} = -\alpha\sigma(U - U_p), T = 1 \quad \text{at} \quad \eta = 1, \tag{26}$$

$$\frac{\partial U}{\partial \eta} = \alpha\sigma(U - U_p), T = 0 \quad \text{at} \quad \eta = -1, \tag{27}$$

$$\frac{\partial^2 U}{\partial \eta^2} = 0 \qquad at \qquad \eta = \pm 1, \tag{28}$$

where $a = \frac{h}{l}$ is the couple stress parameter, $l = \sqrt{\frac{\lambda}{\mu}}$ is the material constant characterizing the couple stress property of the fluid, $M^2 = \frac{B_0^2\sigma_0 h^2}{\mu}$ is the square of the Hartmann number, $G = \frac{\beta' g N h^4}{\nu^2 P_x}$ is the Grashof number, $E_c = \frac{v_0^2 P_x^2}{h^2 C_p(T_1 - T_0)}$ is the Eckert number, $Pr = \frac{\mu C_p}{K_T}$ is the Prandtl number, $\sigma = \frac{h}{\sqrt{k}}$ is the porous parameter, ν is the kinematic viscosity, $Re = \frac{\rho(\frac{\nu P_x}{h})h}{\lambda}$ is the Reynolds number, P_x is the positive values of G correspond to heating along the channel walls.

3. Method of Solution

Velocity and Temperature Distribution

Region 1: Fluid Film

Equation (22) is a fourth order differential equation with constant coefficient, we get the complementary function(CF) as

$$CF = C_1 e^{m_1 \eta} + C_2 e^{-m_1 \eta} + C_3 e^{m_3 \eta} + C_4 e^{-m_3 \eta},$$

and the particular integral(PI) as

$$PI = \frac{1 - G\eta}{M^2},$$

We obtain $U(\eta)$ as the sum of CF and PI, applying the boundary conditions (13) to (15), the velocity of blood are obtained as

$$U(\eta) = C_1 e^{m_1 \eta} + C_2 e^{-m_1 \eta} + C_3 e^{m_3 \eta} + C_4 e^{-m_3 \eta} + \frac{1 - G\eta}{M^2}. \tag{29}$$

Applying the boundary conditions (13) and (14) using equation (9), the temperature of blood is obtained as

$$\begin{aligned} T = {} & C_6\eta + C_5 + I_4 I_5 e^{2\eta m_1} + I_4 I_6 e^{2\eta m_3} \\ & - I_4 I_7 \left(C_2 C_3 e^{\eta(m_3 - m_1)} + C_1 C_4 e^{\eta(m_1 - m_3)} \right) \\ & + I_4 I_9 e^{-2\eta m_1} - I_4 I_8 \left(C_1 C_3 e^{\eta(m_1 + m_3)} + C_2 C_4 e^{\eta(-(m_1 + m_3))} \right) \\ & + I_4 \left(-a^2\eta^4 G^2 M^2 + 4a^2\eta^3 G M^2 - I_{11}\eta^2 + I_4 I_{10} e^{-2\eta m_3} \right) \\ & + I_{12} I_4 \left(C_1 e^{\eta m_1} \left(GM^2 (\eta m_1 - 2) + G m_1^2 - m_1 M^2 \right) \right) \\ & + I_4 C_2 e^{\eta(-m_1)} \left(GM^2 (\eta m_1 + 2) - G m_1^2 - m_1 M^2 \right) \\ & + I_{13} I_4 \left(C_3 e^{\eta m_3} \left(GM^2 (\eta m_3 - 2) + G m_3^2 - m_3 M^2 \right) \right) \\ & + I_4 C_4 e^{\eta(-m_3)} \left(G \left(GM^2 (\eta m_3 + 2) - m_3^2 \right) - m_3 M^2 \right), \end{aligned} \tag{30}$$

where C_1, C_2, C_3, C_4, C_5, C_6, I_4, I_5, I_6, I_7, I_8, I_9 and I_{10} are constants given in the Appendix.

The normalized axial components of velocity obtained from (29) is

$$U' = \frac{U}{\bar{U}},$$

where $\bar{U} = \frac{1}{2}\int_{-1}^{1} U(\eta) d\eta = \frac{(C_1 + C_2)\sinh m_1}{m_1} + \frac{(C_3 + C_4)\sinh m_3}{m_3} + \frac{2}{M^2}.$

Generalized dispersion model

Introducing the non-dimensional quantities

$$\theta = \frac{C}{C_0}; \quad \xi' = \frac{Dx}{h^2\bar{U}}; \quad \xi_s = \frac{Dx_s}{h^2\bar{u}}; \quad \eta = \frac{y}{h}; \quad \tau = \frac{Dt}{h^2}; \quad U = \frac{u}{\bar{u}}; \quad Pe = \frac{h\bar{U}}{D}.$$

equation (10) becomes

$$\frac{\partial\theta}{\partial\tau} + U\frac{\partial\theta}{\partial\xi'} = \frac{1}{Pe^2}\left(\frac{\partial^2\theta}{\partial\xi'^2} + \frac{\partial^2\theta}{\partial\eta^2}\right), \tag{31}$$

We define the axial coordinate moving with the average velocity of flow as $x_1 = x - \tau\bar{U}$ which is in dimensionless form $\xi = \xi' - \tau$, where $\xi = \frac{x_1}{hPe}$. Then, equation (31) becomes

$$\frac{\partial\theta}{\partial\tau} + U'\frac{\partial\theta}{\partial\xi} = \frac{1}{Pe^2}\left(\frac{\partial^2\theta}{\partial\xi^2} + \frac{\partial^2\theta}{\partial\eta^2}\right), \tag{32}$$

where $Pe = \frac{\bar{U}h}{D}$ is the Peclet number and $U' = \frac{U}{\bar{U}}$ (non-dimensional velocity in a moving coordinate system).

The initial and boundary conditions (16) to (18) in dimensionless form are

$$\theta = \begin{cases} 1, |\xi| \leq \frac{\xi_s}{2}, \\ 0, |\xi| > \frac{\xi_s}{2}, \end{cases} \qquad \text{at} \quad \tau = 0, \tag{33}$$

$$\frac{\partial\theta}{\partial\eta} = 0 \qquad \text{at} \qquad \eta = \pm 1, \tag{34}$$

$$\theta = \frac{\partial\theta}{\partial\xi} = 0 \qquad \text{at} \quad \xi = \infty. \tag{35}$$

The solution of equation (32) is obtained using generalized dispersion model of Gill and Sankarasubramanian (1970) is

$$\theta(\tau,\xi,\eta) = \theta_m(\tau,\xi) + f_1(\tau,\eta)\frac{\partial\theta_m}{\partial\xi} + f_2(\tau,\eta)\frac{\partial^2\theta_m}{\partial\xi^2} + ...,$$

that is,

$$\theta(\tau,\xi,\eta) = \theta_m(\tau,\xi) + \sum_{k=1}^{\infty} f_k(\tau,\eta)\frac{\partial^k\theta_m}{\partial\xi^k}, \tag{36}$$

where θ_m is the dimensionless cross sectional average concentration, given by

$$\theta_m(\tau,\xi) = \frac{1}{2}\int_{-1}^{1}\theta(\tau,\xi,\eta)d\eta. \tag{37}$$

Integrating equation (32) with respect to η in $[-1,1]$ and using the equation (37), we get

$$\frac{\partial\theta_m}{\partial\tau} = \frac{1}{Pe^2}\,\frac{\partial^2\theta_m}{\partial\xi^2} + \frac{1}{2}\int_{-1}^{1}\frac{\partial^2\theta}{\partial\eta^2}\,d\eta - \frac{1}{2}\frac{\partial}{\partial\xi}\int_{-1}^{1}U'\,\theta\,d\eta, \tag{38}$$

Substituting equation (36) in (38), we obtain

$$\frac{\partial \theta_m}{\partial \tau} = \frac{1}{P_e^2}\frac{\partial^2 \theta_m}{\partial \xi^2} - \frac{1}{2}\frac{\partial}{\partial \xi}\int_{-1}^{1} U'\left(\theta_m(\tau,\xi) + f_1(\tau,\eta)\frac{\partial \theta_m}{\partial \xi}(\tau,\xi) + \dots\right) d\eta. \tag{39}$$

It is assumed that the process of distributing θ_m is diffusive in nature from the time ero then, following Gill and Sankarasubramanian (1970), the generalized dispersion model for θ_m can be written as

$$\frac{\partial \theta_m}{\partial \tau} = \sum_{i=1}^{\infty} K_i(\tau)\frac{\partial^i \theta_m}{\partial \xi^i}. \tag{40}$$

Substituting the equation (40) in (39) we obtain

$$\begin{aligned} K_1\frac{\partial \theta_m}{\partial \xi} + K_2\frac{\partial^2 \theta_m}{\partial \xi^2} + K_3\frac{\partial^3 \theta_m}{\partial \xi^3} + \dots = \frac{1}{P_e^2}\frac{\partial^2 \theta_m}{\partial \xi^2} - \frac{1}{2}\frac{\partial}{\partial \xi}\int_{-1}^{1} U'(\theta_m(\tau,\xi) \\ + f_1(\tau,\eta)\frac{\partial \theta_m}{\partial \xi} + f_2(\tau,\eta)\frac{\partial^2 \theta_m}{\partial \xi^2}(\tau,\xi) + \dots)d\eta, \end{aligned} \tag{41}$$

Equating the coefficients of $\frac{\partial \theta_m}{\partial \xi}, \frac{\partial^2 \theta_m}{\partial \xi^2}, \dots$ we get,

$$K_i(\tau) = \frac{\delta_{ij}}{P_e^2} - \frac{1}{2}\int_{-1}^{1} U' f_{i-1}(\tau,\eta)d\eta, \quad i = 1,2,3,\dots \text{ and } \ j = 2. \tag{42}$$

where δ_{ij} is the Kroneckar delta defined by

$$\delta_{ij} = \begin{cases} 1, & if \quad i = j, \\ 0, & if \quad i \neq j. \end{cases}$$

Substituting equation (36) in (32), we get

$$\begin{aligned} &\frac{\partial}{\partial \tau}\left(\theta_m(\tau,\xi) + f_1(\tau,\eta)\frac{\partial \theta_m}{\partial \xi}(\tau,\xi) + f_2(\tau,\eta)\frac{\partial^2 \theta_m}{\partial \xi^2}(\tau,\xi) + \dots\right) \\ &+U'\frac{\partial}{\partial \xi}\left(\theta_m(\tau,\xi) + f_1(\tau,\eta)\frac{\partial \theta_m}{\partial \xi}(\tau,\xi) + f_2(\tau,\eta)\frac{\partial^2 \theta_m}{\partial \xi^2}(\tau,\xi) + \dots\right) \\ &= \frac{1}{P_e^2}\frac{\partial^2}{\partial \xi^2}\left(\theta_m(\tau,\xi) + f_1(\tau,\eta)\frac{\partial \theta_m}{\partial \xi}(\tau,\xi) + f_2(\tau,\eta) + \dots\right) \\ &+\frac{\partial^2}{\partial \eta^2}\left(\theta_m(\tau,\xi) + f_1(\tau,\eta)\frac{\partial \theta_m}{\partial \xi} + \dots\right). \end{aligned} \tag{43}$$

Substituting equation (40) in (43), using

$$\frac{\partial^{k+1}\theta_m}{\partial \tau \partial \xi^k} = \sum_{i=1}^{\infty} K_i(\tau)\frac{\partial^{k+i}\theta_m}{\partial \xi^{k+i}},$$

we obtain

$$\left[\frac{\partial f_1}{\partial \tau} - \frac{\partial^2 f_1}{\partial \eta^2} + U' + K_1(\tau)\right]\frac{\partial \theta_m}{\partial \xi} + \left[\frac{\partial f_2}{\partial \tau} - \frac{\partial^2 f_2}{\partial \eta^2} + U' f_1 + K_1(\tau) f_1 + K_2(\tau) - \frac{1}{P_e^2}\right]\frac{\partial^2 \theta_m}{\partial \xi^2} + \sum_{k=1}^{\infty}\left[\frac{\partial f_{k+2}}{\partial \tau} - \frac{\partial^2 f_{k+2}}{\partial \eta^2} + U' f_{k+1} + K_1(\tau) f_{k+1} + \left(K_2(\tau) - \frac{1}{P_e^2}\right) f_k + \sum_{i=3}^{k+2} K_i f_{k+2-i}\right]\frac{\partial^{k+2}\theta_m}{\partial \xi^{k+2}} = 0, \tag{44}$$

with $f_0 = 1$. Equating the coefficients of $\dfrac{\partial^k \theta_m}{\partial \xi^k}$ $(k = 1, 2, 3, \ldots)$ in equation (44) to zero, we obtain the following set of partial differential equations.

$$\frac{\partial f_1}{\partial \tau} = \frac{\partial^2 f_1}{\partial \eta^2} - U' - K_1(\tau), \tag{45}$$

$$\frac{\partial f_2}{\partial \tau} = \frac{\partial^2 f_2}{\partial \eta^2} - U' f_1 - K_1(\tau) f_1 - K_2(\tau) + \frac{1}{P_e^2}, \tag{46}$$

$$\frac{\partial f_{k+2}}{\partial \tau} = \frac{\partial^2 f_{k+2}}{\partial \eta^2} - U' f_{k+1} - K_1(\tau) f_{K+1} - \left(K_2(\tau) - \frac{1}{P_e^2}\right) f_k - \sum_{i=3}^{k+2} K_i f_{k+2-i}. \tag{47}$$

Since θ_m is chosen in such a way to satisfy the initial and boundary conditions on θ, (33) and (34) on f_k function becomes

$$f_k(0, \eta) = 0, \tag{48}$$

$$\frac{\partial f_k}{\partial \eta}(\tau, -1) = 0, \tag{49}$$

$$\frac{\partial f_k}{\partial \eta}(\tau, 1) = 0, \tag{50}$$

for $k = 1, 2, 3, \ldots$

Also, from equation (35) we have

$$\int_{-1}^{1} f_k(\tau, \eta) d\eta = 0, \tag{51}$$

for $k = 1, 2, 3, \ldots$

To find K_i's we know the f_k's and its corresponding initial and boundary conditions. From equation (42) for $i = 1$, using $f_0 = 1$, we get K_1 as

$$K_1(\tau) = 0. \tag{52}$$

From equation (42) for $i = 2$, we get K_2 as

$$K_2(\tau) = \frac{1}{P_e^2} - \frac{1}{2}\int_{-1}^{1} U' f_1 d\eta. \tag{53}$$

To evaluate $K_2(\tau)$,

$$\text{put} \quad f_1 = f_{10}(\eta) + f_{11}(\tau, \eta), \tag{54}$$

where $f_{10}(\eta)$ corresponds to an infinitely wide slug which is independent of τ and f_{11} is $\tau-$ dependent satisfying

$$\frac{df_{10}}{d\eta} = 0 \quad \text{at} \quad \eta = \pm 1, \tag{55}$$

$$\int_{-1}^{1} f_{10} d\eta = 0. \tag{56}$$

Using the (54) in (45) gives

$$\frac{d^2 f_{10}}{d\eta^2} - U' = 0, \tag{57}$$

$$\frac{\partial f_{11}}{\partial \tau} = \frac{\partial^2 f_{11}}{\partial \eta^2}. \tag{58}$$

Solving the equation (57) with conditions (55) and (56) we get

$$f_{10} = \frac{1}{\bar{u}}\left(\frac{C_1 e^{\eta m_1} + C_2 e^{\eta(-m_1)}}{m_1^2} + \frac{C_3 e^{\eta m_3} + C_4 e^{\eta(-m_3)}}{m_3^2} + \left(\frac{1 - \bar{u}M^2}{M^2}\right)\frac{\eta^2}{2} - \frac{\eta^3 G}{6M^2}\right) - C_9\eta - C_{10}. \tag{59}$$

Equation (58) is heat conduction type and its solution satisfying condition $f_{11}(\tau, \eta) = -f_{10}(\eta)$ of the form

$$f_{11} = \sum_{n=1}^{\infty} B_n e^{-\lambda_n^2 \tau} \cos(\lambda_n \eta), \tag{60}$$

$$\text{where} \quad B_n = -2\int_0^1 f_{10}(\eta)\cos(\lambda_n \eta) d\eta, \tag{61}$$

and $\lambda_n = n\pi$. Substituting (59) in (61) we get,

$$B_n = -\frac{1}{\bar{u}}\left(\frac{2(C_1 + C_2)m_1 \cos(n\pi)\sinh(m_1)}{m_1^2(m_1^2 + n^2\pi^2)} + \frac{2(C_3 + C_4)m_3 \cos(n\pi)\sinh(m_3)}{m_3^2(m_3^2 + n^2\pi^2)}\right) + \left(\frac{\bar{u}M^2 - 1}{M^2}\right)\frac{4\cos(n\pi)}{\bar{u}n^2\pi^2}.$$

Substituting (59) and (60) in equation (54) we get,

$$f_1 = \frac{1}{\bar{u}}\left(\frac{C_1 e^{\eta m_1} + C_2 e^{\eta(-m_1)}}{m_1^2} + \frac{C_3 e^{\eta m_3} + C_4 e^{\eta(-m_3)}}{m_3^2} + \left(\frac{1-\bar{u}M^2}{M^2}\right)\frac{\eta^2}{2} - \frac{\eta^3 G}{6M^2}\right) - C_9\eta$$

$$- C_{10} + \frac{e^{-\pi^2\tau}\cos(\pi\tau)}{\pi^3\bar{u}}\left(\frac{2\pi(-1+M^2\bar{u})}{M^2} - \frac{\begin{array}{r}2\pi^3\big((C_3+C_4)(m_1^2+\pi^2)m_1\sin h(m_3)\\ +(C_1+C_2)(m_3^2+\pi^2)m_3\sin h(m_1)\big)\end{array}}{m_1 m_3(m_1^2+\pi^2)(m_3^2+\pi^2)}\right)$$

$$- \frac{e^{-4\pi^2\tau}\cos(2\pi\tau)}{8\pi^3\bar{u}}\left(\frac{4\pi(-1+M^2\bar{u})}{M^2} - \frac{\begin{array}{r}16\pi^3\big((C_3+C_4)(m_1^2+4\pi^2)m_1\sin h(m_3)\\ +(C_1+C_2)(m_3^2+4\pi^2)m_3\sin h(m_1)\big)\end{array}}{m_1 m_3(m_1^2+4\pi^2)(m_3^2+4\pi^2)}\right)$$

$$+ \frac{e^{-9\pi^2\tau}\cos(3\pi\tau)}{27\pi^3\bar{u}}\left(\frac{6\pi(-1+M^2\bar{u})}{M^2} - \frac{\begin{array}{r}54\pi^3\big((C_3+C_4)(m_1^2+9\pi^2)m_1\sin h(m_3)\\ +(C_1+C_2)(m_3^2+9\pi^2)m_3\sin h(m_1)\big)\end{array}}{m_1 m_3(m_1^2+9\pi^2)(m_3^2+9\pi^2)}\right).$$

Substituting f_1 into equation (42) and integrating, we get the solution of dispersion coefficient with help of MATHEMATICA 8.0 where C_9 and C_{10} are constants given in the Appendix.

Similarly, $K_3(\tau)$, $K_4(\tau)$ and so on are obtained and we found that $K_i(\tau), i > 2$ are negligibly small compared to $K_2(\tau)$. Hence, the dispersion model (40) now leads to

$$\frac{\partial\theta_m}{\partial\tau} = K_2\frac{\partial^2\theta_m}{\partial\xi^2}. \tag{62}$$

The exact solution of (62) satisfying the conditions (33) to (36) is obtained using Fourier Transform(Sankara (1995)) as

$$\theta_m(\xi,\tau) = \frac{1}{2}\left[erf\left(\frac{\frac{\xi_s}{2}+\xi}{2\sqrt{T}}\right) + erf\left(\frac{\frac{\xi_s}{2}-\xi}{2\sqrt{T}}\right)\right], \tag{63}$$

where $T = \int_0^\tau K_2(\eta)d\eta$ and $erf(x) = \frac{2}{\sqrt{\pi}}\int_0^x e^{-z^2}dz$.

The flow and heat transfer characteristics are the local skin friction coefficient C_f and the local rate of heat transfer coefficient. Define

$$C_f = \frac{2\tau_1}{\rho(\frac{\nu P_x}{h})^2},\ Nu = \frac{qh}{K_T(T_1-T_0)}, \tag{64}$$

where, $\tau_1 = \mu \left(\frac{\partial u}{\partial y}\right)\Big|_{y=\pm h}$ is the wall shear stress and $q = -K_T \left(\frac{\partial T^*}{\partial y}\right)\Big|_{y=\pm h}$ is the heat flux between the fluid and the wall.

By use of dimensionless quantities equation (64) can be written as:

$$C_f = \frac{2}{Re}\frac{\partial U}{\partial \eta}\bigg|_{\eta=\pm 1}, Nu = \frac{\partial T}{\partial \eta}\bigg|_{\eta=\pm 1}, \tag{65}$$

where Nu is the Nusselt number.

4. Results and Discussion

Dispersion of solute in combined free and forced convective fully developed flow of a couple stress fluid bounded by porous beds under the influence of magnetic field is studied using generalized dispersion model. The results are obtained to illustrate the influence of the Hartmann number $(M = 1, 1.5, 2)$, Grashof number $(Gr = 0, 1, 2)$, couple stress parameter $(a = 1, 20)$, dimensionless time $(\tau = 0.06, 0.3, 0.6, 0.8)$ and porous parameter $\sigma = (60, 120, 200)$ on the velocity, temperature, skin friction coefficient, Nusselt numbers, dispersion coefficient and the concentration profiles, while the values of some of the physical parameters are taken as constant such as $Pr = 100, Ec = 0.2, \alpha = 0.1$ and $\beta_1 = 0.1$ in all the figures. We have extracted interesting insights regarding the influence of all the parameters that govern this problem. The influence of the parameters M, Gr, a, τ and σ on horizontal velocity, temperature, skin friction coefficient, Nusselt numbers, dispersion coefficient and concentration profiles are analyzed from Figures 2 to 21.

The expression for velocity profiles U are evaluated using equation (29) and are shown in Figures 3 and 4 for different values of the Grashof number (Gr) and couple stress parameter (a) with η. It is seen that the effect of increasing Grashof number and couple stress parameter decreases the velocity profile of the blood flow, and are parabolic in nature. Figures 2 and 5 for different values of M and σ with η, reveal that the velocity profile decreases with the increase of the Hartmann number (M) and porous parameter (σ). The effect of M on the velocity profile is displayed. The presence of magnetic field normal to the flow in an electrical conducting fluid introduces a Lorentz force which acts against the flow. This resistive force tends to slow down the blood flow and hence, the boundary layer decreases with the increase of the magnetic field.

The expression for temperature distribution T are evaluated using equation (30) and are shown in Figures 6 and 9 for different values of M and σ with η. It is observed that , temperature of the blood increases with decrease of the value of M and σ. Figures 7 and 8 for different values of Gr and a with η, show that temperature profile increases with increase of Grashof number and couple stress parameter. It is also seen that the temperature is parabolic in nature, increasing from its value at $\eta = -1$ to a maximum temperature around 3.2 and then, decreasing steadily to its value at $\eta = 1$.

The expression for dispersion coefficient $K_2 - Pe^{-2}$ are numerically evaluated using equation (42)

and are shown in Figures 10 to 13 for different values of M, Gr, a and σ with dimensionless time τ. Figure 10 shows that $K_2(\tau) - Pe^{-2}$ decreases with increase in M. From Figures 11 to 13 reveal that the axial dispersion coefficient increases $K_2(\tau) - Pe^{-2}$ with the increase of Grashof number, couple stress and porous parameter which reflects the existence of larger velocity variation across the channel. The effects of above parameters on $K_2(\tau) - Pe^{-2}$ is very significant, when τ is very small and its effect is not so significant for large value of τ. For the values of $Gr \geq 2$, it has been observed that $K_2(\tau) - Pe^{-2}$ reaches a fixed value. That is, where $Gr \geq 2$, $K_2(\tau) - Pe^{-2}$ becomes $\tau-$ independent.

The expression for mean concentration θ_m are numerically evaluated using equation (63) and are shown in Figures 14 to 18 for different values of M, Gr, a, σ and τ with axial distance ξ. Figures 15 to 17 reveal that there is marked variation of concentration with axial distance. It is apparent from these figures that the effect of increasing Gr, a and σ is to decrease the peak value of the mean concentration. This implies that the concentration is more distributed in $\xi-$direction for larger and larger values of Gr. The curves are bell shaped and symmetrical about the origin. θ_m increases with the decrease of the values of M and τ as shown in Figures 14 and 18. These results are useful to understand the transport of solute at different times.

Figure (19) depicts that the effect of skin friction coefficient against M for different values of Grashof number on the lower $(\eta = -1)$ and upper $(\eta = 1)$ wall. It shows that the shear stress grows rapidly for increasing the Grashof number at the lower and upper wall. C_f decreases at the lower wall and increases at the upper wall. Negative values show that flow reversal arises within the boundary layer. The variation of Nusselt number with M is depicted in Figure 20 and in Figure 21. It is observed that the Nusselt numbers decrease with an increase in Grashof number at both the walls $\eta = -1$ and $\eta = 1$.

5. Conclusion

An analysis is carried out to study the heat and mass transfer flow of couple stress fluids between two parallel channels bounded by porous beds and the density is dependent on temperature. When there is a uniform axial temperature variation along the walls, the primary flow shows incipient flow reversal at the upper plate for an increase in temperature along that plate. Similarly flow reversal at the lower plate occurs with a decrease in temperature along that plate. The magnetic field, arising as a body couple in the governing equations is shown to increase the axis dispersion coefficient.

Acknowledgments

The authors are grateful to the learned referees for their useful technical comments and valuable suggestions, which led to a improvement of the paper.

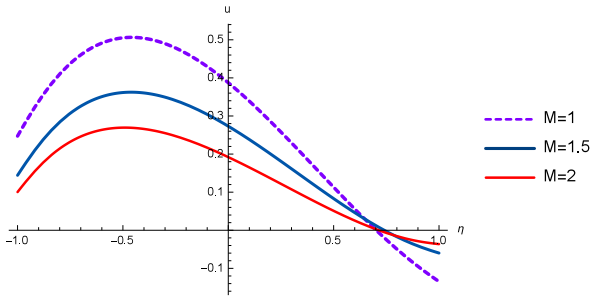

Figure 2. Plots of velocity U versus η for different values of M

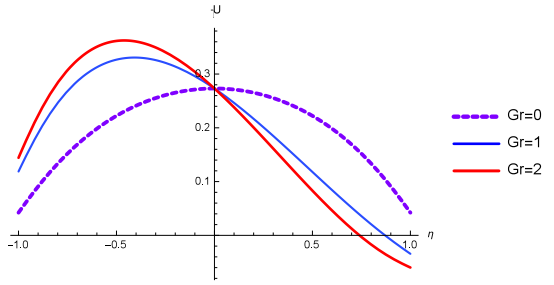

Figure 3. Plots of velocity U versus η for different values of Gr

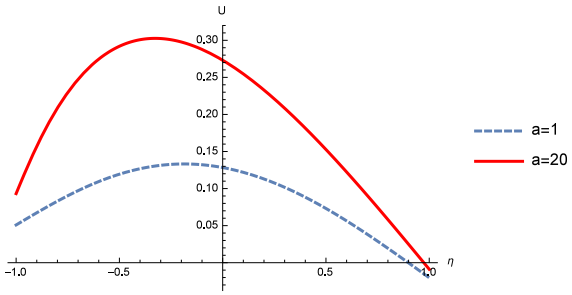

Figure 4. Plots of velocity U versus η for different values of a

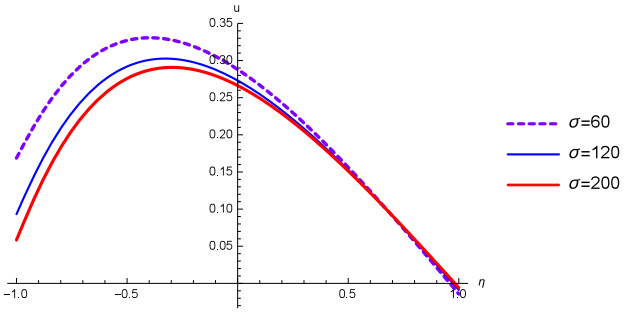

Figure 5. Plots of velocity U versus η for different values of σ

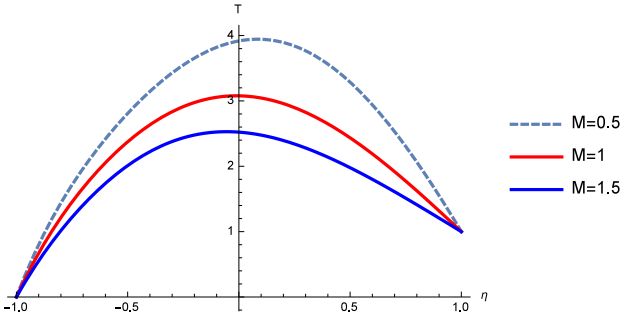

Figure 6. Plots of temperature T versus η for different values of M

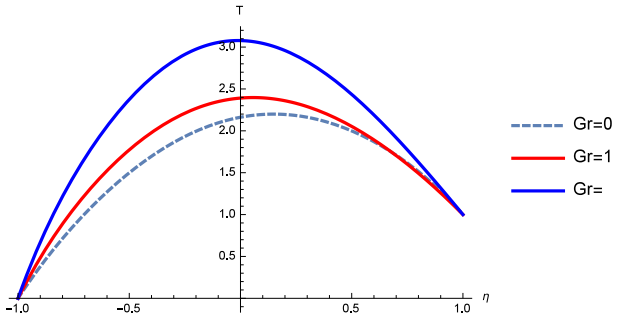

Figure 7. Plots of T versus η for different values of Gr

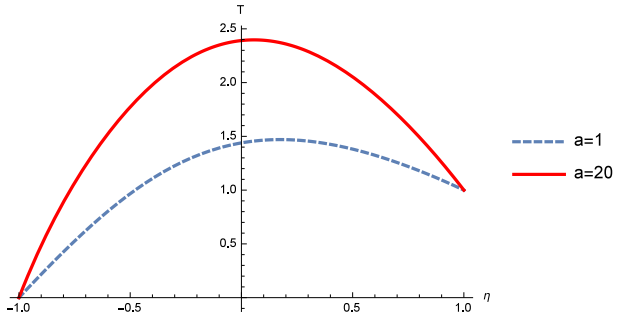

Figure 8. Plots of T versus η for different values of a

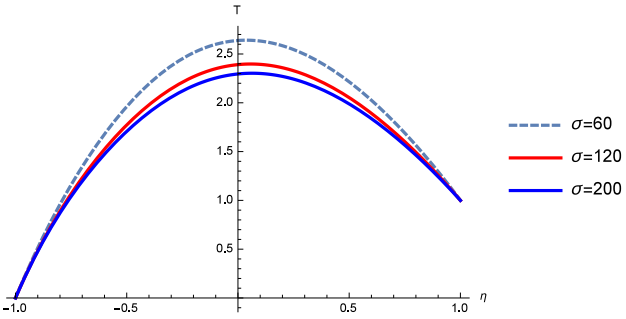

Figure 9. Plots of T versus η for different values of σ

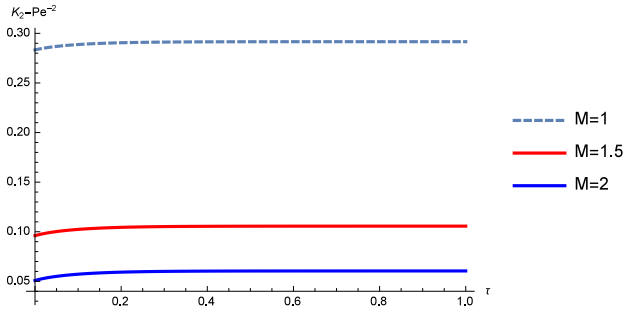

Figure 10. Variation of $K_2(\tau) - Pe^{-2}$ with τ for different values of M

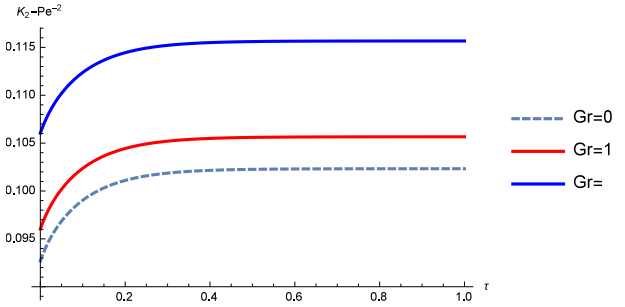

Figure 11. Variation of $K_2(\tau) - Pe^{-2}$ with τ for different values of Gr

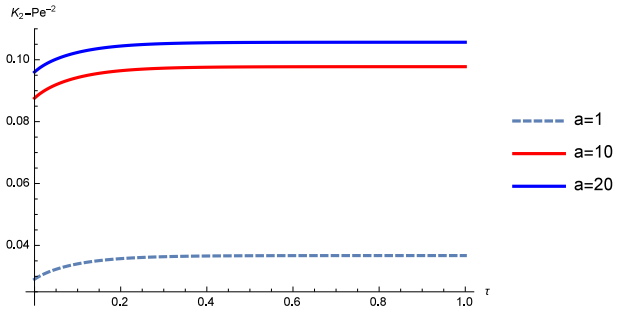

Figure 12. Variation of $K_2(\tau) - Pe^{-2}$ with τ for different values of a

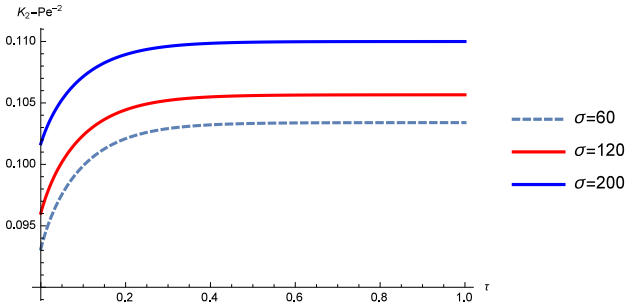

Figure 13. Variation of $K_2(\tau) - Pe^{-2}$ with τ for different values of σ

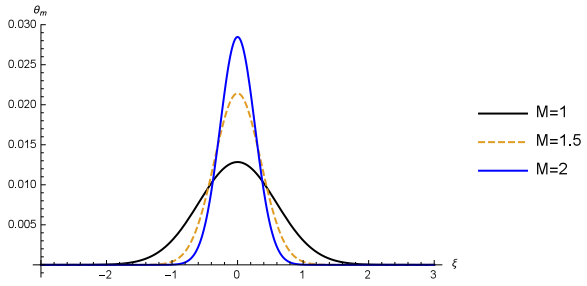

Figure 14. Plots of θ_m versus ξ for different values of Hartmann number M

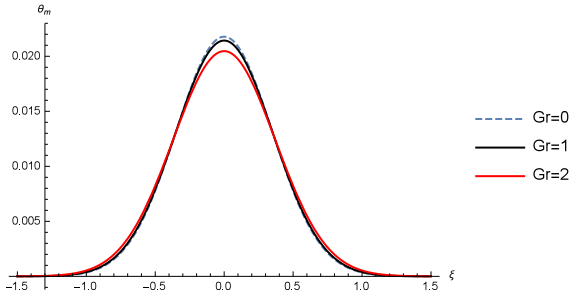

Figure 15. Plots of θ_m versus ξ for different values of Grashof number Gr

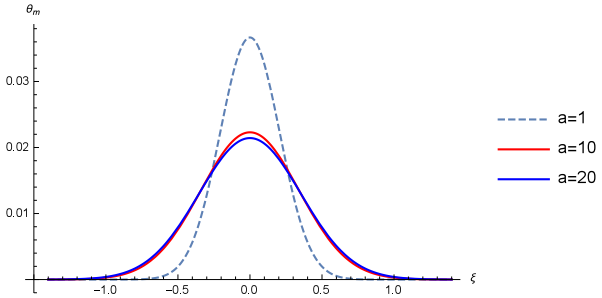

Figure 16. Plots of θ_m versus ξ for different values of couple stress parameter a

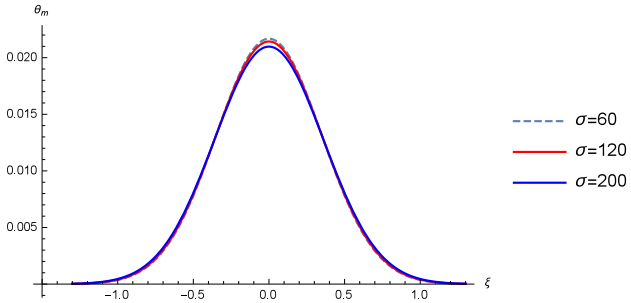

Figure 17. Plots of θ_m versus ξ for different values of porous parameter σ

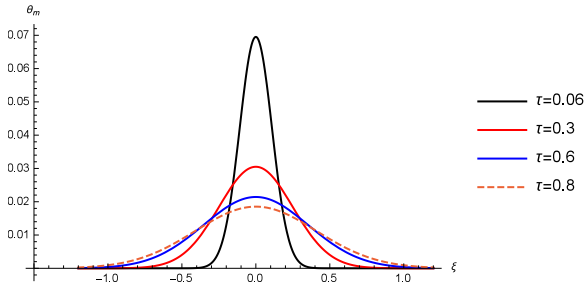

Figure 18. Plots of θ_m versus ξ for different values of time τ

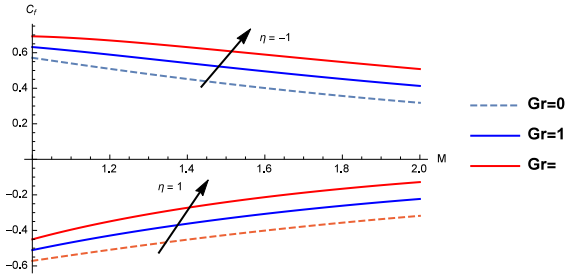

Figure 19. Plots of C_f versus M for different values of Gr

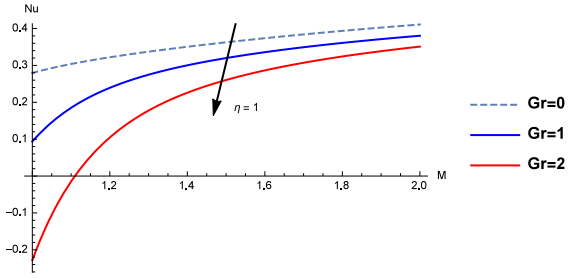

Figure 20. Plots of Nu versus M at $\eta = 1$ for different values of Gr

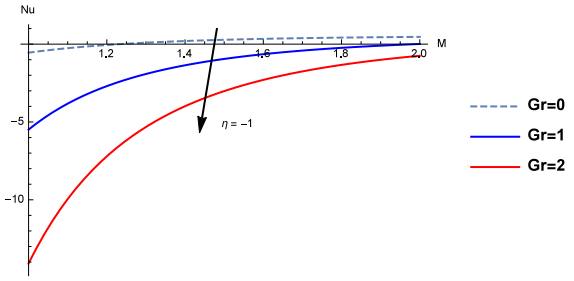

Figure 21. Plots of Nu versus M at $\eta = -1$ for different values of Gr

REFERENCES

Aris, R. (1956). On the dispersion of a solute in a fluid flowing through a tube, Proc. Roy. Soc. Lond. A, Vol. 235, pp. 67-77.

Barton, N. G. (1986). Solute Dispersion and Weak Second-Order Recombination at Large Times in Parallel Flow, J. Fluid Mech, Vol. 164, pp. 289.

Barton, N.G. and Stokes, A.N. (1986). A computational method for shear dispersion in parallel flow, Computational Techniques and Applications, Vol. 85, pp. 345-355.

Beavers, G.S. and Joseph, D.D. (1967). Boundary conditions at a naturally permeable wall, J. Fluid, Vol. 30, pp. 197-207.

Bestman, A.R. (1983). Low Reynolds number flow in a heated tube of varying section, Australian Mathematical Society, Series B., Vol. 25, pp. 244-260.

Bhuvaneswari, M. and Sivasankaran, S. (2014). Free convection flow in an inclined plate with variable thermal conductivity by scaling group transformations , Proceedings of the $21st$ National Symposium on Mathematical Sciences (SKSM21), AIP Conference Proceedings, Vol. 1605, pp. 440-445.

Chatwin, P. C. (1971). On the interpretation of some longitudinal dispersion experiments, Jour. Fluid Mech., Vol. 48, pp. 689-702.

Chinyoka, T. and Makinde, O.D. (2015). Unsteady and porous media flow of reactive non-Newtonian fluids subjected to buoyancy and suction/injection, International Journal of Numerical Methods in Heat and Fluid Flow, Vol. 25, No. 7, pp. 1682704.

Cramer, K.R. and Pai, S.I. (1973). *Magnetofluid dynamics for engineers and applied physicists*, Scripta Publishing Company, Washington D.C.

Erdogan, E. M. and Chatwin, P.C. (1967). The effects of curvature and buoyancy on the laminar dispersion of solute in a horizontal tube, Journal of Fluid Mechanics, Vol. 29, pp. 465-484.

Gill, W. N. and Sankarasubramanian, R. (1970). Exact analysis of unsteady convective diffusion, Proc. Roy. Soc. Lond. A, Vol. 316 , pp. 341-350.

Hughes, W.F. and Young, F.J. (1996). *The electromagnetodynamics of fluids*, 1st edition, Wiley Inc, New York.

Lighthill, M. J. (1966). Initial development of diffusion in Poiseuille flow, J. Inst. Maths. Applics., Vol. 2, pp. 97-108.

Makinde, O.D. Khan, W.A. and Khan, Z.H. (2013). Buoyancy effects on MHD stagnation point flow and heat transfer of a nanofluid past a convectively heated stretching/shrinking sheet, International Journal of Heat and Mass Transfer, Vol. 62, pp. 526-533.

Mazumder, B.S. (1979). Dispersion of solutes in combined free and forced convective flow through a channel, Acta Mechanica, Vol. 32, No. 4, pp. 211-216.

Rashidi, M.M., Momoniat, E. and Rostami, B. (2012), Analytic approximate solutions for MHD boundary-layer viscoelastic fluid flow over continuously moving stretching surface by Homotopy Analysis Method with two auxiliary parameters, Journal of Applied Mathematics, Vol. 2012, pp. 1-19.

Rudraiah, N., Pal, D. and Siddheshwar, P. G. (1986). Effect of couple stresses on the unsteady convective diffusion in fluid flow through a channel, Biorheology, Vol. 23, No. 4, pp. 349-58.

Rundora, L. and Makinde, O.D. (2015). Effects of Navier slip on unsteady flow of a reactive variable viscosity non-Newtonian fluid through a porous saturated medium with asymmetric convective boundary conditions. Journal of Hydrodynamics, Ser. B, Vol. 27, No. 6, pp. 934-944.

Sankar., R. (1995). *Introduction to partial differential equations*, Prentice-Hall of India.

Sankarasubramanian, R. and Gill, W. N. (1973). Unsteady convective diffusion with interphase mass transfer, Proceedings of the Royal Society of London. Series A, Vol. 333, pp. 115-132.

Sekar, R. and Raju, R. (2013). Effect of magnetic field dependent viscosity on Soret-driven thermoconvective instability of ferromagnetic fluid in the presence of rotating anisotropic porous medium of sparse particle suspension, International Journal of Mathematical Sciences, Vol. 12, pp. 13-31.

Sibanda, P. and Makinde, O.D. (2010). On steady MHD flow and heat transfer past a rotating disk in a porous medium with ohmic heating and viscous dissipation, International Journal of Numerical Methods for Heat and Fluid Flow, Vol. 20, No. 3, pp. 269-285.

Siddheshwar, P.G. and Thangaraj, R.P. (2005). Dispersion of solute in a fully developed flow of a Boussinesq Stokes suspension, Hydrodynamics VI - Theory and applications - Cheng and Yeow (eds.), Taylor and Francis Group, London, pp. 483-488.

Sivasankaran, S. (2007). Effect of variable thermal conductivity on buoyant convection in a cavity with internal heat generation, Nonlinear Analysis: Modelling and Control, Vol. 12, No. 1, pp. 113-122.

Srinivasacharya, D., Srinivasacharyulu, N. and Odelu, O. (2011). Flow of couple stress fluid between two parallel porous plates, IAENG International Journal of Applied Mathematics, Vol. 41, No. 2, pp. 10-14.

Kafoussias, N.G., Tzirtzilakis, E.E. and Raptis, A. (2008). Free-forced convective boundary-layer flow of a biomagnetic fluid under the action of a localized magnetic field, Canadian Journal of Physics, Vol. 86, pp. 447-457.

Tzirtzilakis, E.E., Kafoussias, N.G. and Raptis, A. (2010). Numerical study of forced and free convective boundary layer flow of a magnetic fluid over a flat plate under the action of a localized magnetic field, Journal of Applied Mathematics and Physics (ZAMP), Vol. 61, No. 5, pp. 929-947.

Appendix

$$m_1 = \frac{\sqrt{a^2+\sqrt{a^4-4a^2M^2}}}{\sqrt{2}}, \qquad m_3 = \frac{\sqrt{a^2-\sqrt{a^4-4a^2M^2}}}{\sqrt{2}},$$
$$a_3 = e^{m_1}\left(\alpha\sigma + m_1\right), \qquad a_4 = e^{-m_1}\left(m_1 - \alpha\sigma\right),$$
$$a_5 = e^{m_3}\left(\alpha\sigma + m_3\right), \qquad a_6 = e^{-m_3}\left(m_3 - \alpha\sigma\right),$$
$$a_8 = m_1^2 e^{m_1}, \qquad a_9 = m_1^2 e^{-m_1},$$
$$a_{10} = m_3^2 e^{m_3}, \qquad a_{11} = m_3^2 e^{-m_3},$$

$$\begin{aligned} C_1 = -\frac{1}{I_3}(&I_1a_3a_{10}^2 + I_2a_4a_{10}^2 - I_1a_5a_8a_{10} + I_1a_6a_9a_{10} - I_2a_6a_8a_{10} + I_2a_5a_9a_{10} \\ &- I_1a_{11}^2a_3 - I_1a_{11}a_6a_8 + I_1a_5a_9a_{11} - I_2a_{11}^2a_4 - I_2a_{11}a_5a_8 + I_2a_6a_9a_{11}), \end{aligned}$$

$$\begin{aligned} C_2 = -\frac{1}{I_3}(&I_1a_4a_{10}^2 + I_2a_3a_{10}^2 - I_1a_6a_8a_{10} + I_1a_5a_9a_{10} - I_2a_5a_8a_{10} + I_2a_6a_9a_{10} - I_1a_{11}^2a_4 \\ &- I_1a_{11}a_5a_8 + I_1a_6a_9a_{11} - I_2a_{11}^2a_3 - I_2a_{11}a_6a_8 + I_2a_5a_9a_{11}), \end{aligned}$$

$$\begin{aligned} C_3 = -\frac{1}{I_3}(&I_1a_5a_8^2 + I_2a_6a_8^2 + I_1a_3\left(-a_{10}\right)a_8 + I_1a_4a_{11}a_8 - I_2a_{10}a_4a_8 + I_2a_3a_{11}a_8 \\ &- I_1a_5a_9^2 - I_1a_{10}a_4a_9 + I_1a_3a_9a_{11} - I_2a_6a_9^2 - I_2a_{10}a_3a_9 + I_2a_4a_9a_{11}), \end{aligned}$$

$$\begin{aligned} C_4 = -\frac{1}{I_3}(&I_1a_6a_8^2 + I_2a_5a_8^2 - I_1a_{10}a_4a_8 + I_1a_3a_{11}a_8 - I_2a_{10}a_3a_8 + I_2a_4a_{11}a_8 - I_1a_6a_9^2 \\ &- I_1a_{10}a_3a_9 + I_1a_4a_9a_{11} - I_2a_5a_9^2 - I_2a_{10}a_4a_9 + I_2a_3a_9a_{11}), \end{aligned}$$

$$C_5 = \tfrac{1}{2}\left(-q_1 - q_2\right),$$
$$C_6 = \tfrac{1}{2}\left(q_1 - q_2\right),$$
$$C_9 = \tfrac{1}{\bar{u}}\left(\tfrac{(C_1 - C_2\cosh m_1)}{m_1} + \tfrac{(C_3 - C_4\cosh m_3)}{m_3} - \tfrac{G}{2M^2}\right),$$
$$C_{10} = -\left(\tfrac{1-\bar{u}M^2}{6M^2} + \tfrac{(C_1 + C_2\sinh m_1)}{m_1^3} + \tfrac{(C_3 + C_4\sinh m_3)}{m_3^3}\right),$$
$$I_1 = \alpha\sigma\left(\tfrac{1-G}{M^2} - u_p\right),$$
$$I_2 = \alpha\sigma\left(\tfrac{G+1}{M^2} - u_p\right),$$

$$\begin{aligned} I_3 =& a_5^2a_8^2 - a_6^2a_8^2 - 2a_{10}a_3a_5a_8 - 2a_{11}a_3a_6a_8 + 2a_4a_6a_{10}a_8 + 2a_4a_5a_{11}a_8 - a_{11}^2a_3^2 - a_{10}^2a_4^2 \\ &- a_5^2a_9^2 + a_6^2a_9^2 + a_3^2a_{10}^2 + a_4^2a_{11}^2 - 2a_{10}a_4a_5a_9 - 2a_{11}a_4a_6a_9 + 2a_3a_6a_9a_{10} + 2a_3a_5a_9a_{11}, \end{aligned}$$

$$I_4 = \tfrac{\mathrm{Ec\,Pr}}{12a^2M^4},$$
$$I_5 = -\tfrac{3C_1^2M^4\left(a^2\left(m_1^2+M^2\right)+m_1^4\right)}{m_1^2},$$
$$I_6 = -\tfrac{3C_3^2M^4\left(a^2\left(m_3^2+M^2\right)+m_3^4\right)}{m_3^2},$$
$$I_7 = \tfrac{24M^4\left(a^2\left(M^2-m_1m_3\right)+m_1^2m_3^2\right)}{(m_1-m_3)^2},$$
$$I_8 = \tfrac{24M^4\left(a^2\left(m_1m_3+M^2\right)+m_1^2m_3^2\right)}{(m_1+m_3)^2},$$
$$I_9 = -\tfrac{6C_2^2M^4\left(a^2\left(m_1^2+M^2\right)+m_1^4\right)}{2m_1^2},$$

$$I_{10} = -\frac{6C_4^2M^4\left(a^2\left(m_3^2+M^2\right)+m_3^4\right)}{2m_3^2},$$

$$\begin{aligned} I_{11} =& 6a^2\left(-2M^4\left(C_1C_2m_1^2+C_3C_4m_3^2\right)+2\left(C_1C_2+C_3C_4\right)M^6+G^2+M^2\right) \\ &+12M^4\left(C_1C_2m_1^4+C_3C_4m_3^4\right), \end{aligned}$$

$$\begin{aligned} I_{12} &= \frac{24a^2M^2}{m_1^3}, \\ I_{13} &= \frac{24a^2M^2}{m_3^3}, \\ I_{14} &= \frac{EcPr}{12M^4a^2}, \end{aligned}$$

$$\begin{aligned} q_1 =& I_{14}\left(\frac{24a^2C_2e^{m_1}M^2\left(G\left(\left(2-m_1\right)M^2-m_1^2\right)-m_1M^2\right)}{m_1^3}-a^2G^2M^2-4a^2GM^2\right) \\ &+\frac{24I_{14}a^2C_1e^{-m_1}M^2\left(G\left(\left(-m_1-2\right)M^2+m_1^2\right)-m_1M^2\right)}{m_1^3} \\ &+\frac{I_{14}C_4e^{m_3}\left(24a^2M^2\left(G\left(\left(2-m_3\right)M^2-m_3^2\right)-m_3M^2\right)\right)}{m_3^3} \\ &+\frac{I_{14}C_3e^{-m_3}\left(24a^2M^2\left(G\left(\left(-m_3-2\right)M^2+m_3^2\right)-m_3M^2\right)\right)}{m_3^3} \\ &+6I_{14}e^{2(m_1+m_3)}M^4\left(-\frac{C_2^2e^{-2m_3}\left(a^2\left(m_1^2+M^2\right)+m_1^4\right)}{2m_1^2}-\frac{C_4^2e^{-2m_1}\left(a^2\left(m_3^2+M^2\right)+m_3^4\right)}{2m_3^2}\right) \\ &-I_{14}I_8\left(C_1C_3e^{-m_1-m_3}+C_2C_4e^{m_1+m_3}\right)-I_7I_{14}\left(C_2C_3e^{m_1-m_3}+C_1C_4e^{m_3-m_1}\right) \\ &+I_5I_{14}e^{-2m_1}+I_5I_{14}e^{-2m_3}-I_{11}I_{14}, \end{aligned}$$

$$\begin{aligned} q_2 =& -1+I_{14}\left(-a^2G^2M^2+4a^2GM^2+I_5e^{2m_1}\right) \\ &+\frac{24I_{14}a^2C_1e^{m_1}M^2\left(G\left(\left(m_1-2\right)M^2+m_1^2\right)-m_1M^2\right)}{m_1^3} \\ &+\frac{24I_{14}a^2C_2e^{-m_1}M^2\left(G\left(\left(m_1+2\right)M^2-m_1^2\right)-m_1M^2\right)}{m_1^3} \\ &-I_7I_{14}\left(C_2C_3e^{m_3-m_1}+C_1C_4e^{m_1-m_3}\right)-I_8I_{14}\left(C_1C_3e^{m_1+m_3}+C_2C_4e^{-m_1-m_3}\right) \\ &+I_{14}I_6e^{2m_3}+\frac{I_{14}C_3e^{m_3}\left(24a^2M^2\left(G\left(\left(m_3-2\right)M^2+m_3^2\right)-m_3M^2\right)\right)}{m_3^3} \\ &+\frac{I_{14}C_4e^{-m_3}\left(24a^2M^2\left(G\left(\left(m_3+2\right)M^2-m_3^2\right)-m_3M^2\right)\right)}{m_3^3}-I_{11}I_{14} \\ &+6I_{14}e^{-2(m_1+m_3)}M^4\left(-\frac{C_2^2e^{2m_3}\left(a^2\left(m_1^2+M^2\right)+m_1^4\right)}{2m_1^2}-\frac{C_4^2e^{2m_1}\left(a^2\left(m_3^2+M^2\right)+m_3^4\right)}{2m_3^2}\right). \end{aligned}$$